Magneto-optical Kerr spectroscopy of noble metals

L. Uba,[1] S. Uba,[1] and V. N. Antonov[1,2]

[1]*Faculty of Mathematics and Informatics, University of Bialystok, K. Ciolkowskiego 1M, PL-15-245 Bialystok, Poland*

[2]*G. V. Kurdyumov Institute for Metal Physics of the N.A.S. of Ukraine, 36 Vernadsky Street, 03142 Kiev, Ukraine*

(Received 7 August 2017; revised manuscript received 24 November 2017; published 20 December 2017)

Magneto-optical (MO) response of the noble metals Cu, Ag, and Au in the joint experimental and *ab initio* theoretical study is reported. The magneto-optical polar Kerr effect (MOKE) spectra of the noble-metal films were measured with the high sensitivity in the applied magnetic field of 1.5 T over the photon energy range 0.74–5.8 eV. Complete set of the optical conductivity tensor elements was determined precisely from the MOKE and the optical spectra measured at the same energy points. The importance of the off-diagonal intraband Drude-type transitions is demonstrated explicitly for each noble metal and found to be a substantial contribution to the observed spectra. It is shown that the first-principles calculations using the spin-polarized fully relativistic Dirac linear-muffin-tin-orbital method with the inclusion of correlation effects by GGA+U approach reproduce well the experimental spectra and allow to explain the microscopic origin of the noble metals' magneto-optical response in terms of interband transitions. Although the energy band structures of Cu, Ag, and Au are very similar, there are some distinctive differences in bandwidths and the energy positions of the bands (especially in X and L symmetry points), mainly due to different spin-orbit splitting and differences in the spatial extent of $3d$, $4d$, and $5d$ valence wave functions of noble metals. It was found that the small differences in the band positions lead to significant differences in the MO properties of three noble metals. Although the spin-orbit interaction in Au is about six times larger than in Cu, and approximately two times larger than in Ag, the absolute value of Kerr rotation in Au is of the same magnitude as in Cu and one order of magnitude smaller as compared to Ag. The sharp Kerr effect spectral peak in Ag is not due to the electronic interband transitions, but rather to the plasma-edge splitting. The band-by-band decomposition of the Cu, Ag, and Au MO spectra is presented and the interband transitions responsible for the prominent structures in the spectra are identified. It has been found that main magneto-optical activity of noble metals in external magnetic field originates from interband transitions at well-defined small-volume regions of Brillouin zone located near the "neck" and "belly" of the Fermi surface.

DOI: 10.1103/PhysRevB.96.235132

I. INTRODUCTION

Noble metals assume a special status because of their practical importance in optoelectronic and nano-optical devices, and their role as model systems for the study of the elementary electronic excitations that underlie the interaction of electromagnetic fields with metals. The measurement of the optical spectra of noble metals is quite challenging with the values of dielectric function spanning over five orders of magnitude from the mid-infrared to the visible/ultraviolet spectral range. Although the optical properties of noble metals are widely investigated both experimentally and theoretically (see, for example, Refs. [1,2] for Cu and Ag and Refs. [3,4] for Au, see also Ref. [5] and references therein), there are quite a few experimental papers devoted to the magneto-optical (MO) properties of the noble metals [6–10]. Faraday rotation and circular dichroism in Cu and Au thin metal films was measured in Ref. [9] in the mid-infrared (0.112–0.136 eV) spectral interval. The MO Kerr effect (MOKE) in pure Ag and Au in the visible and near-infrared region of the spectrum (1.13 to 3.1 eV) has been measured by McGroddy *et al.* [6]. The spectral dependence of the Kerr rotation and Kerr ellipticity in the photon energy range of 2 to 5.5 eV was investigated experimentally by Schnatterly [7] for all noble metals. In Ref. [7], only Kerr ellipticity spectra were measured while the Kerr rotation ones were calculated using Kramers-Kronig relationships. The optical and MO properties of evaporated and sputtered Ag were studied experimentally by Deng *et al.* [10]. The simulations of Kerr spectra, based on the classical Drude model, were presented. Several authors investigated spin injection from a ferromagnet to a nonmagnetic metal by measuring the time-resolved polar MOKE of Cu, Ag, and Au [11–13] without external magnetic field. Recently, Berritta *et al.* [14] presented *ab initio* theory of the magnetization induced by circularly polarized laser light in noble metals. They showed that the induced magnetization is strongly materials and frequency dependent, and demonstrated the existence of both spin and orbital induced magnetizations which exhibit a significantly different behavior.

We should mention that due to nonmagnetic ground state of noble metals, the magneto-optical Kerr effect can be observed only in an external magnetic field. The experimental measurement of the MOKE spectra of noble metals is challenging due to extremely small signal.

The calculations of the energy band structure of noble metals also have a long story. For example, early works on the band structure of gold from the 1970s [15,16] focused on relativistic effects which are responsible for its yellow color and has been used as a reference to interpret photoemission experiments. It was found that the cohesive energy in noble metals contains large terms arising from dispersion forces, such as van der Waals interactions [17], pointing to the importance of many-body correlations for closed-shell d electrons. The band structure of Au, calculated by density functional theory (DFT) within the local density approximation (LDA) or the generalized gradient approximation (GGA), presents an underestimation of the $5d$-$6sp$ interband gap by $\sim$1.0 eV with respect to the available experimental data. To solve

these disagreements, quasiparticle (QP) corrections to the DFT eigenvalues have been applied with success [18–22].

This paper presents the original experimental and detailed theoretical investigation of the MO properties of diamagnetic noble metals Cu, Ag, and Au induced by an external magnetic field. Investigations of the electronic structure and optical properties of metals in external magnetic fields are important for understanding of fundamental concepts in quantum theory of solids [23,24]. We present the magneto-optical polar Kerr effect spectra of the fcc noble-metal films measured with the high sensitivity in the applied magnetic field of 1.5 T over the photon energy range 0.74–5.8 eV. From the measured optical and MOKE spectra, a complete set of the optical conductivity tensor elements was determined and compared with *ab initio* spin-polarized relativistic linear-muffin-tin-orbital (LMTO) calculations. To our best knowledge, the magneto-optical properties of the noble metals have not been investigated theoretically from the first principles yet. From the detailed analysis of the interband transitions responsible for the noble metals MOKE spectra, it has been found that in spite of the well-known similarities of many electronic properties of Cu, Ag, and Au metals, the subtle differences of their electronic band structure result in the individual behavior of the MO response of these metals.

The paper is organized as follows. The description of the experimental procedure and theoretical framework is provided in Sec. II. Section III presents the experimental and theoretical MO spectra of the noble metals in the external magnetic field. Theoretical analysis of electronic structure and MO properties of the noble metals is presented. Finally, the results are summarized in Sec. IV.

II. EXPERIMENTAL AND THEORETICAL DETAILS

A. Magneto-optical properties

Phenomenologically, magneto-optical effects at optical frequencies are treated by means of the optical conductivity tensor. In the polar geometry, where the z axis is chosen to be perpendicular to the solid surface, and parallel to the magnetization direction, the expression for the complex Kerr angle is given by [25]

$$\theta_K(\omega) + i\varepsilon_K(\omega) = \frac{-\sigma_{xy}(\omega)}{\sigma_{xx}(\omega)\sqrt{1 + \frac{4\pi i}{\omega}\sigma_{xx}(\omega)}}, \tag{1}$$

with θ_K the Kerr rotation and ε_K the Kerr ellipticity. $\sigma_{\alpha\beta}$ ($\alpha,\beta \equiv x,y,z$) is the optical conductivity tensor, which is related to the dielectric tensor $\varepsilon_{\alpha\beta}$ through

$$\varepsilon_{\alpha\beta}(\omega) = \delta_{\alpha\beta} + \frac{4\pi i}{\omega}\sigma_{\alpha\beta}(\omega). \tag{2}$$

Here and henceforth, the following definitions have been adopted. We choose the time dependence of the electric field as $\exp(-i\omega t)$. Hence, all the complex quantities are expressed by their real and imaginary parts as follows: $\sigma_{\alpha\beta} = \sigma^{(1)}_{\alpha\beta} + i\sigma^{(2)}_{\alpha\beta}$, $\varepsilon_{\alpha\beta} = \varepsilon^{(1)}_{\alpha\beta} + i\varepsilon^{(2)}_{\alpha\beta}$, where $\varepsilon_{xx} = (n + ik)^2$, and n and k are refractive index and extinction coefficient, respectively.

The optical conductivity tensor components or, equivalently, the dielectric tensor are the basic spectral quantities of the medium and can be evaluated from the optical and Kerr effect measurements [26]. The complex optical conductivity tensor components for the metals can be separated into two terms

$$\sigma_{\alpha\beta}(\omega) = \sigma^{\text{inter}}_{\alpha\beta}(\omega) + \sigma^{\text{intra}}_{\alpha\beta}(\omega), \tag{3}$$

where $\sigma^{\text{inter}}_{\alpha\beta}(\omega)$ and $\sigma^{\text{intra}}_{\alpha\beta}(\omega)$ are the so-called interband and intraband contributions, respectively. For the diagonal tensor components, both terms are important and should be considered simultaneously. The intraband contribution to the off-diagonal optical conductivity is very small and usually neglected in the case of magnetically ordered materials. For metals which have zero spontaneous exchange splitting, the level splitting induced by an external magnetic field available in the experiment is small and the contributions of intraband and interband transitions to the off-diagonal optical conductivity tensor component become comparable. Therefore, the intraband term should be taken into account on the same footing as the interband one [24].

The usual way to incorporate the intraband contribution to the optical conductivity tensor is to use the Drude model [27]. The classical equation of motion for a free electron in a magnetic field, with a damping constant $\gamma_D = \tau_D^{-1}$, where τ_D is a phenomenological Drude electron relaxation time, gives the following expressions for the intraband contributions to the diagonal $\sigma^D_{xx}(\omega)$ and off-diagonal $\sigma^D_{xy}(\omega)$ parts of the optical conductivity tensor [25,26]:

$$\sigma^D_{xx}(\omega) = \frac{\omega_p^2}{4\pi}\frac{(\gamma_D - i\omega)}{(\gamma_D - i\omega)^2 + \omega_c^2}, \tag{4}$$

$$\sigma^D_{xy}(\omega) = \frac{\omega_p^2}{4\pi}\frac{\omega_c}{(\gamma_D - i\omega)^2 + \omega_c^2}, \tag{5}$$

with ω_p being the plasma frequency, $\omega_p^2 = 4\pi e^2 n^2/m^*$, where n is the carrier concentration. ω_c is cyclotron frequency

$$\omega_c = eB/m^*c, \tag{6}$$

where B is the applied magnetic field, e is the electron charge, $m^* = m(1 + \lambda)$ is the effective mass of the carrier, renormalized in solids by the electron-phonon interaction constant λ.

To apply the formula (5), suitable values of the parameters are needed. As a first approximation, zero-frequency values taken from dc-transport measurements can be used. The $\sigma^D_{xx}(\omega)$ and $\sigma^D_{xy}(\omega)$ conductivities for $\omega = 0$ are

$$\sigma^D_{xx}(0) = \frac{1}{\varrho}, \tag{7}$$

$$\sigma^D_{xy}(0) = -\frac{\varrho_H}{\varrho^2}, \tag{8}$$

where ϱ and ϱ_H are dc and Hall resistivity, respectively [25,26].

On the other hand, from the expressions (4) and (5) the following formulas for $\sigma^D_{xx}(0)$ and $\sigma^D_{xy}(0)$ can be obtained for $\gamma_D \gg \omega_c$:

$$\sigma^D_{xx}(0) = \frac{\omega_p^2}{4\pi}\frac{1}{\gamma_D}, \tag{9}$$

$$\sigma^D_{xy}(0) = \frac{\omega_p^2}{4\pi}\frac{\omega_c}{\gamma_D^2}. \tag{10}$$

From the comparison of the formulas (7) and (9) and (8) and (10), the γ_D can be expressed as

$$\gamma_D = \frac{\varrho}{|\varrho_H|}\omega_c. \tag{11}$$

The effect of an external magnetic field on the band structure can be accounted for by including to the Hamiltonian the Zeeman term

$$H_Z = \mu_B(\hat{l} + 2\hat{s})B, \tag{12}$$

which couples spin $\hat{s}$ and orbital $\hat{l}$ moments of an electron to the external magnetic field B. In this work, the band structure of the noble metals in an external magnetic field was calculated self-consistently with the matrix elements of the Zeeman term (12) included to the Hamiltonian matrix of the LMTO method at the variational step.

The optical conductivity of the noble metals has been computed from the energy band structure by means of the Kubo-Greenwood linear-response expression [28,29]

$$\sigma_{\alpha\beta}(\omega) = \frac{-ie^2}{m^2\hbar V_{uc}} \times \sum_{\mathbf{k}}\sum_{nn'} \frac{f(\epsilon_{n\mathbf{k}}) - f(\epsilon_{n'\mathbf{k}})}{\omega_{nn'}(\mathbf{k})} \frac{\Pi^{\alpha}_{n'n}(\mathbf{k})\Pi^{\beta}_{nn'}(\mathbf{k})}{\omega - \omega_{nn'}(\mathbf{k}) + i\gamma}, \tag{13}$$

where $f(\epsilon_{n\mathbf{k}})$ is the Fermi function, $\hbar\omega_{nn'}(\mathbf{k}) \equiv \epsilon_{n\mathbf{k}} - \epsilon_{n'\mathbf{k}}$ is the energy difference of the Kohn-Sham energies, and γ is the inverse lifetime parameter, which is included to describe the finite lifetime of the excited Bloch electron states. The $\Pi^{\alpha}_{nn'}$ are the dipole optical transition matrix elements, which in a fully relativistic description are given by

$$\mathbf{\Pi}_{nn'}(\mathbf{k}) = m\langle\psi_{n\mathbf{k}}|c\boldsymbol{\alpha}|\psi_{n'\mathbf{k}}\rangle \tag{14}$$

with $\psi_{n\mathbf{k}}$ being the four-component Bloch electron wave function and $\boldsymbol{\alpha}$ are the Dirac matrices. The combined correction terms were also taken into account in the optical matrix element calculations [30]. The detailed description of the optical matrix elements in the Dirac representation is given in Ref. [3]. We mention, lastly, that the absorptive part of the optical conductivity was calculated in a wide energy range and then the Kramers-Kronig transformation was used to calculate the dispersive parts of the optical conductivity from the absorptive ones. The plasma frequency ω_p in Eqs. (4) and (5) was calculated using the expression

$$(\omega_p)^2 \equiv \frac{4\pi e^2}{m^2 V_{uc}} \sum_{n\mathbf{k}} \delta(\epsilon_{n\mathbf{k}} - E_F)|\Pi_{nn}|^2, \tag{15}$$

where E_F is the Fermi energy.

In systems without spontaneous polarization, as diamagnetic metals, such as Cu, Ag, and Au, the effect of the external field is twofold: to split the double-degenerate states by a certain amount of energy, the Zeeman splitting, and to induce diamagnetic current. The first term is included in our calculations but the second contribution is ignored. Grechnev *et al.* [31] show that diamagnetic current in noble metals is smaller than the Zeeman term by at least two orders of magnitude.

B. Experimental details

To study the magneto-optical response of the noble metals, we measured the polar MOKE spectra of the Cu, Ag, and Au films at room temperature in the external magnetic field of 1.5 T aligned normally to the film plane over the photon energy range $0.74 \leqslant \hbar\omega \leqslant 5.8$ eV. Thick (∼2000 Å) polycrystalline fcc Cu, Ag, and Au films were prepared on 0.5-mm-thick glass substrates using dc sputtering deposition system. The polar Kerr effect induced in the noble metals by the magnetic field of 1.5 T is very small (below 2×10^{-3} deg in Cu and Au) and was detected in a sensitive Kerr spectrometer setup [32] by means of the polarization modulation technique using a piezobirefringent modulator. Aside from the high sensitivity reaching the 10^{-5}–10^{-4} deg range (depending on the photon energy and corresponding photon shot noise), this method has the advantage that the Kerr rotation and Kerr ellipticity can be determined simultaneously. The resulting complex Kerr rotation values were determined as a half of the difference of the signals measured with the magnetic field of 1.5 T switched alternately between the positive and negative values. Acquisition time was long enough to obtain sufficiently large signal-to-noise ratio. The precise calibration procedure of the Kerr rotation and ellipticity was performed before the measurements. The measurements were repeated a number of times and the resulting spectra presented in the paper were obtained by averaging over all the measurements. The optical properties were measured directly on the same samples by conventional spectroscopic ellipsometry using the rotating analyzer method over the same spectral range as for the MOKE spectra.

C. Calculation details

The details of the computational method are described in our previous papers [33–38], and here we only mention several aspects. The calculations were performed using the spin-polarized fully relativistic linear-muffin-tin-orbital (SPR LMTO) method [39,40] in the atomic sphere approximation (ASA) with the combined correction term taken into account. Our implementation of the LMTO method uses four-component basis functions constructed by solving the Dirac equation inside an atomic sphere [41]. The LSDA part of the calculations was based on the spin-density functional with the Perdew-Wang [42] exchange-correlation potential. The exchange-correlation functional of a GGA type was also used in the version of Perdew, Burke, and Ernzerhof [43]. Brillouin zone (BZ) integrations were performed using the improved tetrahedron method [44] until the charge self-consistency was achieved. The MO spectra of noble metals in the external magnetic field are extremely small in amplitude and to reproduce them theoretically, we have to use a very fine mesh in the BZ. We used in our MO calculations the mesh in the k space of $200 \times 200 \times 200$, which gives 676 800 irreducible $\mathbf{k}$ points and 4 000 000 tetrahedra. The basis consisting of s, p, d, and f LMTO's was used. Core-charge densities were recalculated at every iteration of the self-consistency loop. To compare the theoretically calculated optical spectra with the experimentally ones, we have convoluted the calculated spectra with a Lorentzian with selected widths γ to approximate a lifetime broadening.

TABLE I. Parameters used in the calculations of the optical and magneto-optical spectra of Cu, Ag, and Au noble metals in comparison with available experimental data. The β_s and β_l parameters were used to multiply the spin and orbital Zeeman terms [Eq. (12)].

Parameter	Method	Cu	Ag	Au
ω_p (eV)	Our results	8.3	9.5	8.4
	Expt. [45]	8.8	9.0	9.0
	Expt. [2]		8.9	
	Expt. [4]			8.45
γ (eV)	Our results	0.1	0.02	0.1
γ_D (eV)	Our results	0.05	0.07	0.05
	Expt. [45]	0.144	0.020	0.071
	Expt. [2]		0.039	
	Expt. [4]			0.047
ω_c (eV)	Our results	-8.1×10^{-5}	-9.0×10^{-5}	-10.8×10^{-5}
β_s	Our results	-1.0	-1.0	-1.0
β_l	Our results	0.55	0.25	0.55

Table I presents the final values of the parameters used in the calculations of the optical and magneto-optical spectra of Cu, Ag, and Au noble metals in comparison with available experimental data [2,4,45]. To take into account the intraband contribution to the MO properties of the noble metals, the phenomenological Drude-type model has been adopted in this work. To use the Drude model in the form of Eqs. (4) and (5), we need three parameters: the plasma frequency ω_p, the cyclotron frequency ω_c, and the damping constant γ_D. The approximate values of the first two parameters were calculated using Eqs. (15) and (6). To estimate the renormalized effective electron mass m^* we used the constant of the electron-phonon interaction $\lambda = 0.07$, 0.04, and 0.12, respectively, for Cu, Ag, and Au calculated in the rigid muffin-tin (MT) approximation in Refs. [46–48]. The inverse intraband Drude relaxation time γ_D can be estimated from the dc and Hall resistivity data using the expression (11). Such an estimation using the values of $\varrho = 10.8 \times 10^{-6}$ [Ω cm] and $\varrho_H = 3.3 \times 10^{-9}$ [Ω cm] (at 300 K in the magnetic field of 1.5 T) taken from Ref. [49] gives $\gamma_D = 0.05$ eV for Au. Similar estimations produce the $\gamma_D = 0.05$ eV and 0.075 eV for Cu and Ag, respectively.

The noble-metal band structure, calculated by density functional theory within the local density approximation or the generalized gradient approximation, presents an underestimation of the $5d$-$6sp$ interband gap by $\sim$1.0 eV with respect to the available experimental data. To solve these disagreements, more advanced methods might be used, such as LSDA plus self-interaction corrections [50], the LSDA+U [51] method, GW approximation [52], or dynamical mean-field theory [53–55]. Among them, the LSDA+U method is the simplest and most frequently used. We used in this work the "relativistic" generalization of the rotationally invariant version of LSDA+U method [56] which takes into account spin-orbit (SO) coupling so that the occupation matrix of localized electrons becomes nondiagonal in spin indexes. This method is described in detail in our previous paper [56] including the procedure to calculate the screened Coulomb U and exchange J integrals, as well as the Slater integrals F^2, F^4, and F^6.

The screened Coulomb U and exchange J integrals enter the LSDA+U energy functional as external parameters and have to be determined independently. These parameters can be determined from supercell LSDA calculations using Slater's transition state technique [57,58], from constrained LSDA calculations (cLSDA) [58–62], or the constrained random-phase approximation (cRPA) scheme [63]. Subsequently, a combined cLSDA and cRPA method was also proposed [64]. The cRPA method, however, is known to yield values of U that are too small in some cases [38]. On the other hand, the cLSDA method produces too large values of U [65]. Therefore, in our calculations we treated the Hubbard U as an external parameter and varied it from 2 to 4 eV. We adjusted the value of U to achieve the best agreement with the experimental spectra. We found that the value of $U_{\text{eff}} = U - J = 2.5$ eV gives the best agreement between the calculated and experimental optical and MO spectra in noble metals.

It should be mentioned that the effect of the Coulomb correlations changes the energy band structure of transition-metal compounds in two ways. First, d occupied states are shifted downward by $U_{\text{eff}}/2$ and empty d states are shifted upward by this amount relative to the Fermi energy. Second, the Coulomb correlations enhance an effective spin-orbit coupling constant [66].

III. EXPERIMENTAL RESULTS AND COMPARISON WITH THE THEORY

A. Optical spectra

Figure 1 shows the calculated real part of the optical conductivity, $\sigma_{1xx}(\omega)$, compared with the experimental data. Overall, the spectral shape of the experimental optical conductivity spectra are qualitatively reproduced by the GGA calculations. However, the positions of the calculated edge of the optical conductivity are shifted towards smaller energies as compared to the experiment in all noble metals. One of the possible reasons is the nonexact treatment of the correlation effects. Indeed, the GGA+U approximation with $U_{\text{eff}} = 2.5$ eV improves the description of the optical conductivity spectra of noble metals not only in the energy position of the main features, but also in the absolute value and the shape of the spectra.

Figure 2 shows the calculated real and imaginary parts of the dielectric function, $\varepsilon_{1xx}(\omega)$ and $\varepsilon_{2xx}(\omega)$, the optical reflectivity R, and the imaginary part of the energy-loss function Im $[-1/\varepsilon(\omega)]$, compared with our measurements for noble metals. On the basis of the results of the GGA+U band structure calculation, the observed optical reflectivity spectra of Cu can be sorted into the respective intraband and interband transition groups: (1) metallic high reflectivity below $\sim$2.2 eV, (2) a steep edge between $\sim$2.1 and $\sim$2.4 eV due to appearance of the interband transitions to the Fermi level, and (3) above the minimum at $\sim$4.2 eV some less pronounced structures with a broad maximum of R between 4.5 and 6 eV. Similar behavior is seen also for Ag and Au.

The predominant structure of noble metals' reflectivity spectra is the edge which is situated at 2.1, 3.7, and 2.5 eV in Cu, Ag, and Au, respectively. This sudden characteristic drop is due to a plasma oscillation interfering with interband

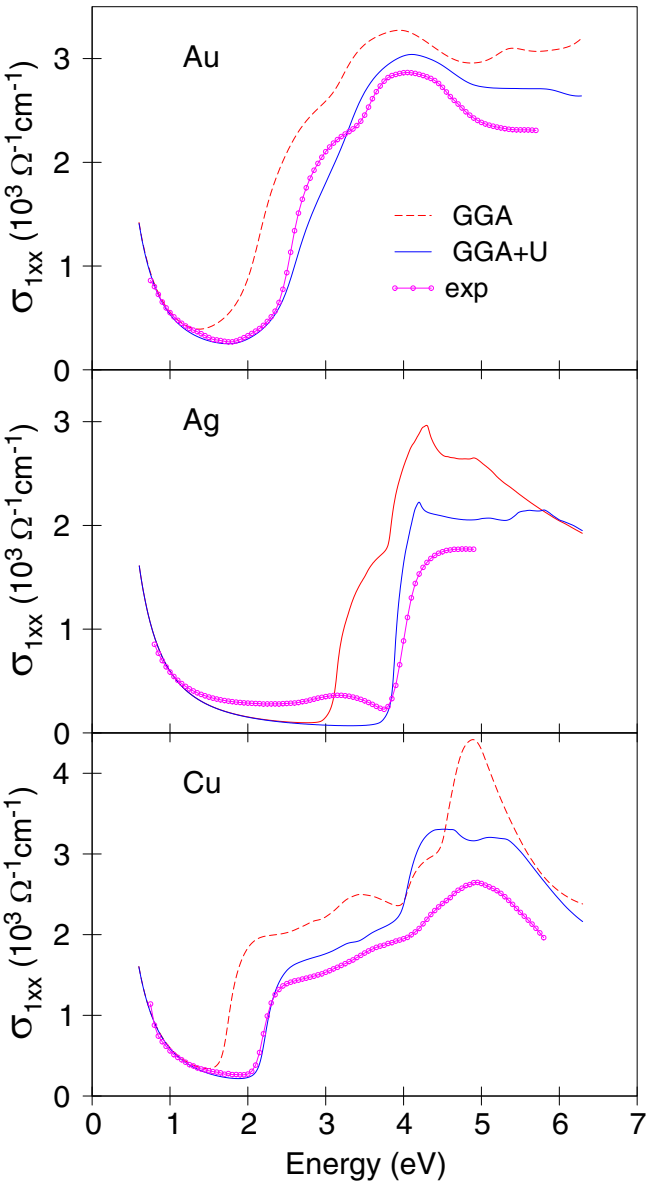

FIG. 1. Comparison between the experimentally measured (circles) optical conductivity σ_{1xx} spectra of noble metals and theoretically calculated in GGA (dashed lines) and GGA+U (solid lines) approximation.

excitations. This plasma resonance causes the correspondent colors of noble metals. The energy of the conduction electron plasma resonance in the presence of the interband excitations is determined by the condition $\varepsilon_{1xx}(\omega) \approx 0$. This condition is almost fulfilled in Ag and, hence, it has the largest peak of the energy-loss spectrum among all noble metals. In Cu, the plasmon peak is much less pronounced. The correct energy position of the plasma edge in noble metals can be obtained only by taking into account the d-d correlation effects.

B. MO Kerr spectra

Figures 3–5 show the experimental MOKE and off-diagonal conductivity $\omega\sigma_{xy}$ spectra of the diamagnetic noble-metal films measured in the magnetic field of 1.5 T (circles) and the

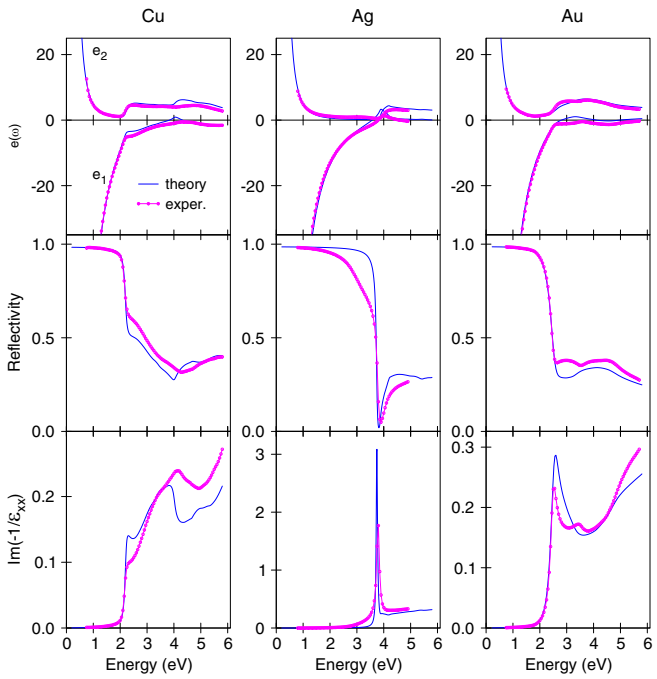

FIG. 2. Comparison between the experimentally measured (circles) optical spectra (the dielectric function ε_{xx}, optical reflectivity R, and the energy-loss function Im $[-1/\varepsilon]$) of noble-metal films and the spectra calculated in the GGA+U approximation (solid lines).

theoretically calculated spectra (solid lines) in the GGA+U approximation including full Zeeman term [Eq. (12)]. The Kerr rotation and ellipticity in the visible spectral range are very small in magnitude and do not overcome the values of $\sim 1.5 \times 10^{-3}$ deg, $\sim 1.1 \times 10^{-2}$ deg, and $\sim 2.5^{-3}$ deg in the field of 1.5 T in copper, silver, and gold, respectively.

The off-diagonal optical conductivity spectra of noble metals have been obtained experimentally using the directly measured Kerr rotation and ellipticity spectra in combination with the measured diagonal optical spectra according to Eq. (1). This is a nontrivial task because to obtain the correct spectra one should measure the MOKE and ε_{xx} spectra with a high spectral resolution in the same energy points to decrease possible errors. The MOKE spectra in Ag have a strong resonance in a very narrow energy interval, and to detect the MOKE and optical spectra we used energy mesh of 5 to 10 meV with spectral resolution of 2 meV. We should also mention that while the sensitivity of the experimental procedure used in this work is very high and generally within 0.005–0.01 m deg range for the Kerr rotation and ellipticity (depending on the photon energy and corresponding photon shot noise), the variances increase significantly (up to ± 0.02 m deg) at the high energy edge of the measured energy interval.

The measured Kerr rotation and ellipticity spectra of Ag have typical resonance structures (Fig. 4). The MOKE spectra of Au have a less pronounced resonance (Fig. 5). On the other hand, the characteristic features of the measured Kerr rotation spectrum of Cu shown in Fig. 3 are a broad maximum in the 2.5 to 5.8 eV spectral range, a prominent minimum at $\sim$2.3 eV, and a flat low-energy shoulder with a small peak at $\sim$2.0 eV.

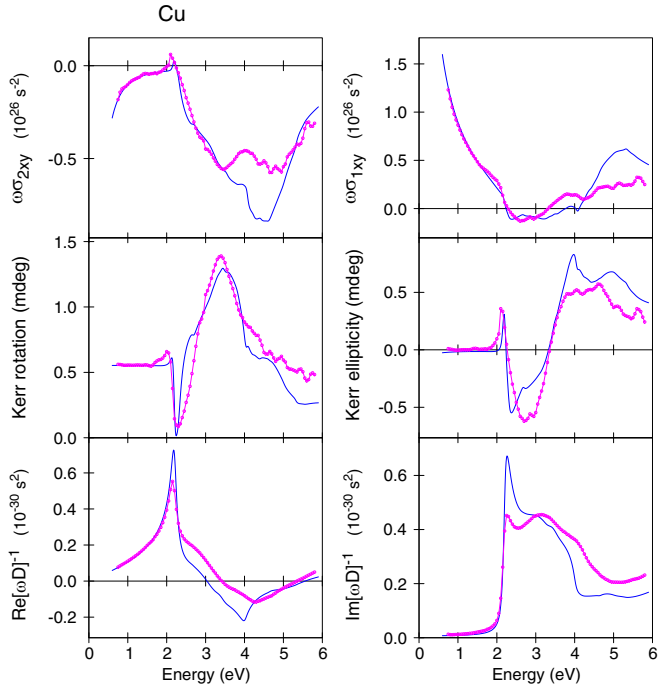

FIG. 3. Comparison between the experimentally measured in the applied field of 1.5 T (circles) and theoretically calculated (solid lines) in GGA+U approximation off-diagonal optical conductivity $\omega\sigma_{xy}$, polar Kerr rotation, and Kerr ellipticity spectra and the imaginary and real parts of the function $[\omega D]^{-1}$ in fcc Cu.

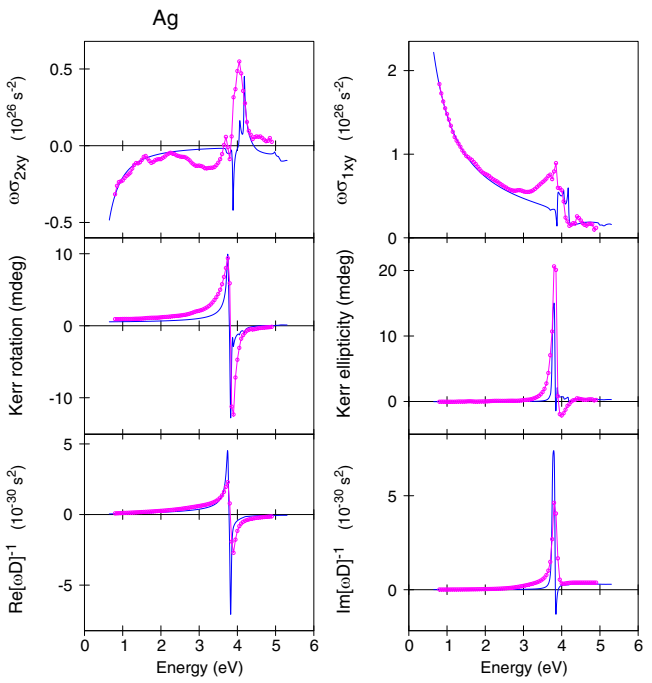

FIG. 4. Comparison between the experimentally measured in the applied field of 1.5 T (circles) and theoretically calculated in GGA+U approximation (solid lines) off-diagonal optical conductivity $\omega\sigma_{xy}$, polar Kerr rotation, and Kerr ellipticity spectra and the imaginary and real parts of the function $[\omega D]^{-1}$ in fcc Ag.

The calculated $\omega\sigma_{xy}$ and MOKE spectra for Cu, Ag, and Au, shown in Figs. 3–5, describe well the experiment and reproduce main features of measured spectra. However, to obtain the best agreement with the experimentally measured MO spectra in the absolute values we have to introduce the parameters β_s and β_l (Table I). The spin and orbital Zeeman terms in Eq. (12) have been multiplied by the β_s and β_l factors, respectively, for all noble metals.

We found that due to the smallness of the spin polarization induced by an external magnetic field, the contributions of intraband and interband transitions to the off-diagonal optical conductivity tensor component become comparable for all noble metals. As a result, frequency-dependent behavior of the off-diagonal optical conductivity in noble metals is greatly affected by intraband optical transitions' contribution. Therefore, the intraband term must be taken into account on the same footing as the interband one. Similar situation was previously encountered in the case of paramagnetic Pt [24]. To take into account the intraband contribution to the MO properties of noble metals, the phenomenological Drude-type model has been adopted in this work. The Drude parameters used are presented in Table I.

We should point out that the contribution of the intraband transitions, Im $[\sigma^D_{xy}(\omega)]$, to the absorptive part of the off-diagonal optical conductivity $\sigma_{2xy}(\omega)$ is proportional to $1/\omega^3$ for $\omega \gg \gamma_D$ and is important only in the IR energy range (see Figs. 3–5). As a consequence, this contribution determines the low-frequency behavior of the $\sigma_{2xy}(\omega)$ spectrum, whereas in the UV-Vis range its effect is relatively small. At the same time, the dispersive part $\sigma_{1xy}(\omega)$ is affected by the off-diagonal Drude term in the whole energy interval studied because the Re $[\sigma^D_{xy}(\omega)]$ decreases only as $1/\omega^2$ at high frequencies. We can conclude that the energy dependence of the off-diagonal optical conductivity as well as the MOKE spectra of noble metals are greatly affected by the contribution coming from the intraband optical transitions.

Although the energy band structures of Cu, Ag, and Au are very similar, there are some distinctive differences in bandwidths and the energy positions of the bands (especially in X and L symmetry points). It is mainly different spin-orbit splitting, different lattice constants, and the difference in the spatial extent of $3d$, $4d$, and $5d$ valence wave functions of noble metals. The small differences in the band positions lead to significant differences in the MO properties of three noble metals. Although the spin-orbit interaction in Au is about six times larger than in Cu, and approximately two times larger than in Ag, the absolute value of Kerr rotation in Au is of the same magnitude as in Cu and one order of magnitude smaller as compared to Ag.

To investigate the origin of the Kerr spectra, we consider the separate contributions of both the numerator of Eq. (1), i.e., $\sigma_{xy}(\omega)$ and the denominator, $\mathrm{D}(\omega) \equiv \sigma_{xx}(1 + \frac{4\pi i}{\omega}\sigma_{xx})^{1/2}$. In Figs. 3–5 we show how the separate contributions of numerator and denominator bring about the complex Kerr angle of noble metals. In Ag, the real part of the inverse denominator (times the photon frequency) Re$[\omega \mathrm{D}]^{-1}$ displays a strong resonance structure at about 3.7 eV. The imaginary part of the off-diagonal optical conductivity spectrum, i.e., $\omega\sigma_{2xy}$, in this metal is a rather small value at that energy. As a result, the shape of the Kerr rotation spectrum in this metal

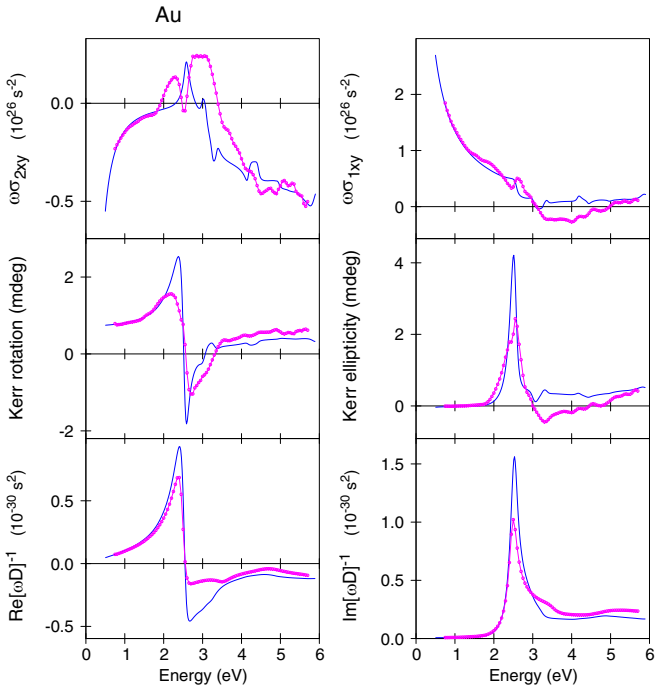

FIG. 5. Comparison between the experimentally measured in the applied field of 1.5 T (circles) and theoretically calculated in GGA+U approximation (solid lines) off-diagonal optical conductivity $\omega\sigma_{xy}$, polar Kerr rotation, and Kerr ellipticity spectra and the imaginary and real parts of the function $[\omega D]^{-1}$ in fcc Au.

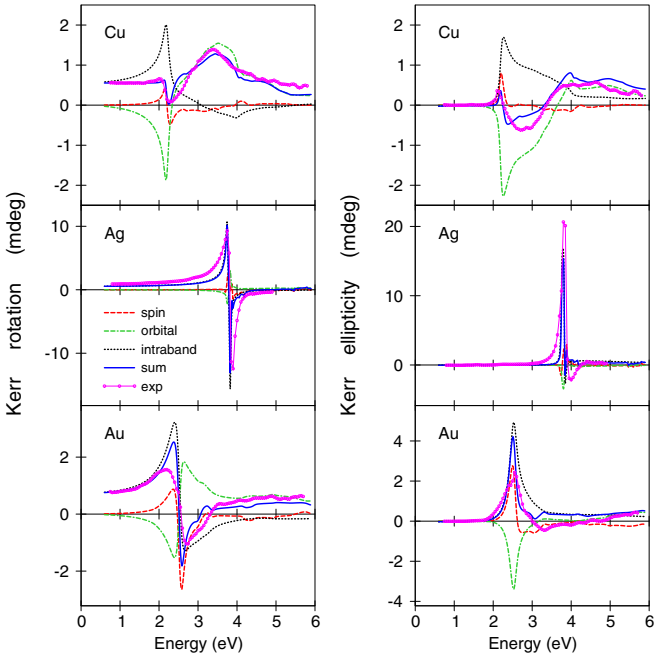

FIG. 6. Decomposition of the theoretically calculated Kerr rotation (left column) and Kerr ellipticity (right column) spectra of noble metals into spin (red dashed lines) and orbital (green dashed-dotted lines) contributions of the Zeeman term [Eq. (12)]. Full lines present the theoretically calculated MO spectra with the orbital contribution reduced by 45%, 75%, and 45% in Cu, Ag, and Au, respectively. The experimentally measured MO spectra in the applied field of 1.5 T are presented by circles. The intraband contributions are shown by black dotted lines.

is almost completely determined by shape of the function Re $[\omega D(\omega)]^{-1}$ in Eq. (1). Also, the shape of the Kerr ellipticity spectrum in Ag is determined by the shape of the function Im $[\omega D(\omega)]^{-1}$. Actually, our first-principles band structure calculations confirm the idea already drawn by Reim and Schoenes in Ref. [25] on the basis of model calculations that the sharp Kerr effect in Ag is not due to the electronic interband transitions, but rather to the influence of a plasma resonance.

The shapes of experimental Kerr rotation and ellipticity spectra of Au are also similar to the shape of the correspondent inverse denominator $[\omega D(\omega)]^{-1}$ (Fig. 5). On the other hand, the shape of Re $[\omega D(\omega)]^{-1}$ and Im $[\omega D(\omega)]^{-1}$ in Cu differs from corresponding Kerr rotation and ellipticity spectra (Fig. 3). Therefore, the MOKE in Cu is a complex function of the inverse denominator $[\omega D(\omega)]^{-1}$ and off-diagonal optical conductivity function $\omega\sigma_{xy}(\omega)$.

C. Contribution of the orbital and spin Zeeman terms

To investigate the origin of the Kerr spectra in noble metals, we consider the separate contributions of both the Zeeman splitting [Eq. (12)] and the spin-orbit (SO) interaction to the MO spectra. We found that the SO interactions are only responsible for the spin part of the Zeeman term, but practically do not contribute to the orbital part of the off-diagonal optical conductivity σ_{xy} in Cu and Ag, and only in small amount, of 10%, in the case of Au.

In Fig. 6 we show the contributions to the Kerr rotation (left column) and Kerr ellipticity (right column) spectra of Cu, Ag, and Au arising from the intraband transitions, as well as the interband transitions coming from orbital $\hat{l}$ and spin $2\hat{s}$ Zeeman terms. The off-diagonal intraband contribution was determined from Eq. (5) with the external parameters ω_c, ω_p, and γ_D. We found that the best agreement between the experimentally measured and theoretically calculated Drude tails in the σ_{1xy} and σ_{2xy} (see Figs. 3–5) was obtained for the parameters ω_c, ω_p, and γ_D listed in Table I.

From our GGA+U calculations it follows that the spin and orbital parts of Zeeman terms give quite different contributions to the Kerr rotation and ellipticity spectra (see Fig. 6). In Cu, the spin and orbital terms contribute to different fine structures in the Kerr rotation spectrum. The spin term mostly contributes to a characteristic small peak at ~2.0 eV, while the orbital term contributes to all the spectral intervals. The GGA+U calculations overestimate the orbital contribution to the Kerr rotation spectra in Cu. To get the best agreement between the calculated and the experimental off-diagonal optical conductivity and Kerr rotation and ellipticity spectra in absolute values, we have to decrease the contribution of the orbital Zeeman term by 45%, 75%, and 45% in Cu, Ag, and Au, respectively. In diamagnetic metals without spontaneous polarization, the effect of the external field is twofold: to split the double-degenerate states by a certain amount of energy, the Zeeman splitting, and to induce diamagnetic current. The first term is included in our calculations, but the second contribution is ignored. Therefore, one of the possible reasons of the reduction of the orbital contribution to the MO spectra of

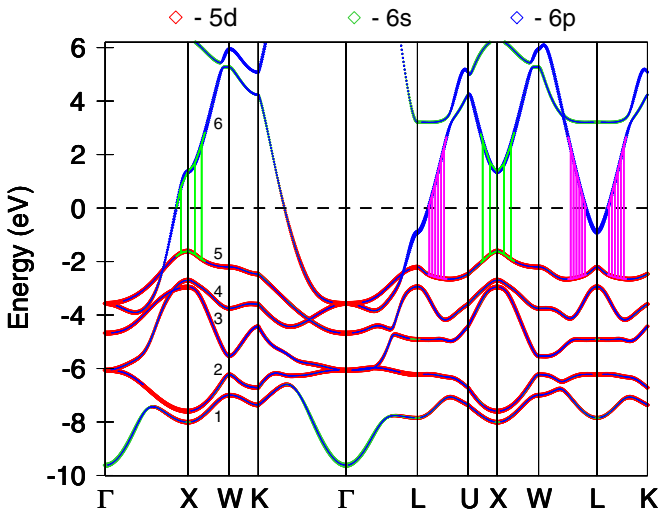

FIG. 7. Energy band structure of Au in fat-band representation. Vertical arrows indicate the most intensive interband transitions in **k** space.

noble metals is the diamagnetic contribution. The situation in Ag differs from Cu and Au. The sharp Kerr effect in Ag is mostly not due to the interband transitions, but to the influence of a strong plasma resonance and is rather well described by the shape of the inverse denominator $[\omega D(\omega)]^{-1}$.

The magnetic moments calculated for magnetic field of 1.5 T are 5.5, 4.1, and 6.2 $\times$ 10^{-5} μ_B for Cu, Ag, and Au, respectively. We found that magnetic moments are the linear function of the external magnetic field with a rate of 3.6 $\times$ $10^{-5}\mu_B$/T, 2.7 $\times$ 10^{-5} μ_B/T, and 4.1 $\times$ $10^{-5}\mu_B$/T for Cu, Ag, and Au, respectively.

It is obvious that the most rigorous approach when an external magnetic field is present would be an implementation of the Larmor and Landau diamagnetism in the band structure, optical, and MO calculations *a priori*. A realization of a nonlocal current-density-functional model would be very interesting to use for studies of the electronic structure and MO properties of noble metals in external magnetic fields.

D. Band-by-band and *k*-space decomposition

To investigate the origin of the MO response of noble metals, we performed detailed analysis of the band-by-band and **k**-space decomposition of the electronic interband transitions in all noble metals. In the absence of magnetic field, due to the time-reversal symmetry, all bands of noble metals are at least twofold degenerate. The external magnetic field lifts the degeneracy. In the following analysis, to distinguish individual bands it will be convenient to keep the numeration of the bands by pairs, adding a subscript if necessary. Thus, for example, the "transition $n \rightarrow m$" means the sum over the four possible interband transitions between the initial pairs of bands $n_{1,2}$ and final pairs of bands $m_{1,2}$. The example of band numbering order in the Brillouin zone for the case of Au is shown in Fig. 7.

The absorptive part of the diagonal optical conductivity tensor element σ_{1xx} and of the off-diagonal part σ_{2xy} are directly connected via Eq. (13) to the microscopic interband optical transitions. As the absorptive parts of the optical conductivity

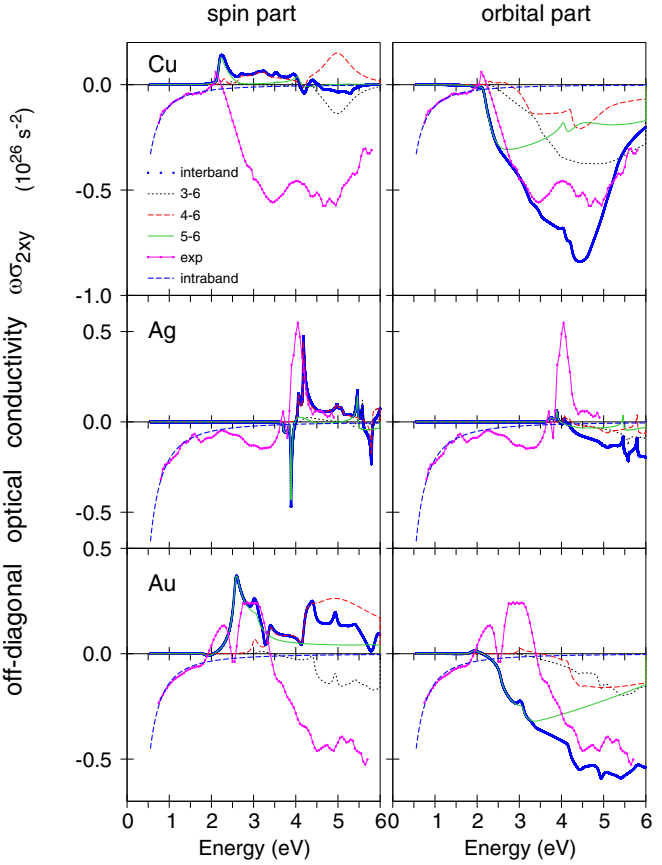

FIG. 8. The experimental off-diagonal $\omega\sigma_{2xy}$ spectra of noble metals (magenta circles) and theoretically calculated contributions (blue circles) from spin- (left column) and orbital-part (right column) interband transitions as well as the contributions from the $3 \rightarrow 6$ (dashed-dotted lines), $4 \rightarrow 6$ (dashed lines), and $5 \rightarrow 6$ (full lines) interband transitions. The blue dashed curves present the intraband contributions.

are additive quantities, to explain the microscopic origin of the MOKE activity of noble metals in terms of individual electronic transitions, we performed the decomposition of the calculated σ_{2xy} spectra into the contributions arising from separate interband transitions (Fig. 8). For better clarity, the intraband contributions are excluded from the calculated σ_{2xy} and shown separately by dashed lines. As it was discussed before, all calculated contributions for Cu, Ag, and Au were multiplied by the corresponding factors β_s and β_l from Table I. Decomposition for the diagonal σ_{1xx} in Au and Cu, Ag can be found in Refs. [67] and [68], respectively.

The experimental off-diagonal optical conductivity spectrum $\omega\sigma_{2xy}$ in Cu has a narrow positive peak at 2.05 eV and a wide negative valley between 3.5 and 5.5 eV (upper row in Fig. 8). We found that the positive peak is completely derived from the spin contribution due to the $5 \rightarrow 6$ interband transitions. On the other hand, the spectrum above 2.2 eV is derived from the orbital contribution due to the $3 \rightarrow 6$, $4 \rightarrow 6$, and $5 \rightarrow 6$ interband transitions. The $\omega\sigma_{2xy}$ in Ag is entirely due to the spin contribution and intraband transitions. The characteristic features of the experimental $\omega\sigma_{2xy}$ spectrum of Au arise from the positive double peak at 2 to 3 eV and negative

structure at 4 to 6 eV. For photon energies up to 6 eV, the $\omega\sigma_{2xy}$ of Au is formed almost entirely by the transitions from the third, fourth, and fifth bands to the sixth band. The initial states for these transitions, bands $3_{1,2}$, $4_{1,2}$, and $5_{1,2}$, are rather narrow bands predominantly of d character (see Fig. 7), while the final states $6_{1,2}$ are wide free-electron-like s-p bands. The intensive double peak in $\omega\sigma_{2xy}$ around 2 to 3 eV is mainly determined by the $5 \rightarrow 6$ with small amount of the $4 \rightarrow 6$ transitions mixed in. The $4 \rightarrow 6$ and $3 \rightarrow 6$ transitions mostly cover 4 to 5.5 eV energy interval. The $4 \rightarrow 6$ and $3 \rightarrow 6$ transitions in the 4 to 5.5 eV range have an opposite sign and compensate each other to some extent.

We should mention that as in the case of spin-part interband transitions, the orbital-part interband transitions in Au are formed almost entirely by the transitions $3,4,5 \rightarrow 6$ for a whole energy interval. However, there is a significant difference between the spin- and orbital-part interband transitions. While most spin-part interband transitions are strongly localized in energy, the orbital-part interband transitions are more smooth functions of energy and cover a whole energy interval for all the $n \rightarrow m$ transitions. In other words, the orbital-part interband transitions take place in all the reciprocal space and cannot be localized in the **k** space. Actually, our first-principles band structure calculations confirm the idea already drawn by Bennet and Stern in Ref. [27] on the basis of the analytical analysis of the MO properties of nonferromagnetic materials that the spin contribution has a frequency dependence which differs from that of the orbital field contribution. The magnetic orbital-part field contribution comes from all the electrons and spread over an energy range of the order of the Fermi energy. The magnetic field spin-part contribution comes from the selected electrons and spread in energy which is quite small compared to the Fermi energy; for these electrons, the MO response energy dependence varies much more strongly than that for the magnetic field orbital contribution.

To see how the interband transitions between the individual bands are located in the reciprocal space of noble metals, we performed the **k**-space decomposition of the spin and orbital interband transitions into transitions occurring in the vicinity of the high-symmetry points of the Brillouin zone. For this aim, we summed all transitions within a specified vicinity surrounding a given point. We found that X and L high-symmetry points of BZ are important only. For X points, the transitions occur within a semisphere which radius is equal to 0.25 of the $\Gamma - X$ distance and a total volume is approximately 3.5% of the whole BZ. We can say that these transitions take place between occupied d and empty p states below and above the "belly" of the Fermi surface, respectively. These transitions give the contributions to spin and orbital parts of the spectra marked with green dashed lines in Fig. 9 and are indicated with green vertical lines in Fig. 7. For the L symmetry points, the transitions occur within a slice of semispheres which the outer and inner radii are equal to 0.40 and 0.15 of the $\Gamma - X$ distance, respectively, and total volume is approximately 20% of whole BZ. These transitions take place between states below and above the "neck" of the Fermi surface, respectively. These transitions give the contributions to spin and orbital parts of the spectra marked with red solid lines in Fig. 9 and are indicated with magenta vertical lines in Fig. 7. As can be seen from Fig. 7, there are no transitions in the nearest vicinity of L points, and all transitions occur within a necklace surrounding the neck of the Fermi surface. These transitions stand for the main contribution to the magneto-optical activity of Au in the UV-Vis spectral range (Fig. 9).

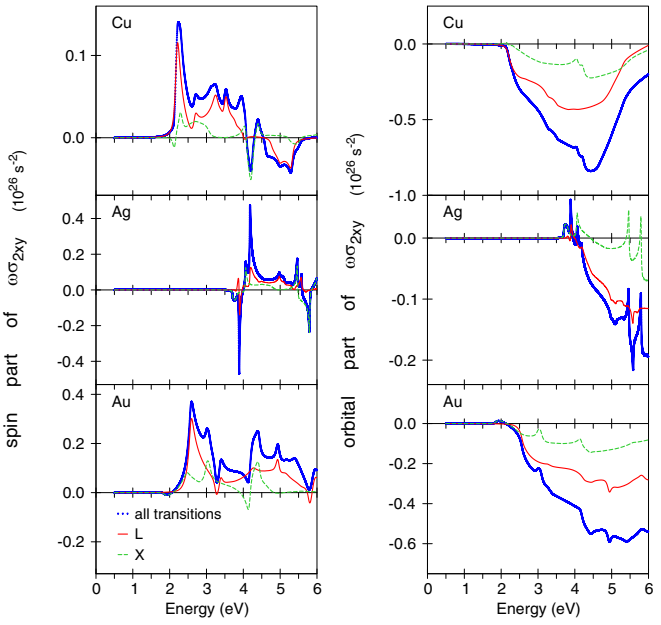

FIG. 9. Contributions of spin- and orbital-part interband transitions to the off-diagonal $\omega\sigma_{2xy}$ spectrum of noble metals from different parts of the BZ (the intraband contributions are neglected). Red and green lines mark the transitions located at vicinities of the L and X symmetry points, respectively. Blue lines describe all interband transitions.

The similar decompositions have been performed for Cu and Ag with the same radii of spheres as for Au. The results are presented in upper and medium panels in Fig. 9. It is clear that all of the above observations and conclusions are relevant for Cu and Ag as well. The main magneto-optical activity of noble metals in the UV-Vis spectral range originates from transitions in the region of Brillouin zone near the "neck" and "belly" of the Fermi surface.

IV. CONCLUSIONS

The magneto-optical response of the diamagnetic noble metals, Cu, Ag, and Au, films measured in the external magnetic field of 1.5 T over the photon energy range $0.74 \leqslant \hbar\omega \leqslant 5.8$ eV is presented. From the data, a complete set of optical conductivity tensor elements spectra over the energy range studied were determined. The band structure and MOKE spectra calculations of the noble metals have been performed by the spin-polarized relativistic LMTO method within GGA+U approximation, with the term $\mu_B B(\hat{l} + 2\hat{s})$ added to the Hamiltonian which couples the spin and orbital moments of electron to the external magnetic field.

It was shown that the frequency-dependent behavior of the off-diagonal optical conductivity is greatly affected by intraband optical transitions' contribution. If the influence of

the intraband transitions on the absorptive part of the optical conductivity tensor $\sigma_{2xy}(\omega)$ manifests mainly in the IR energy range, the dispersive parts of the optical conductivity tensor $\sigma_{1xy}(\omega)$ are affected by the intraband transitions in the whole energy interval studied.

Noble metals belong to strongly correlated systems. Standard GGA cannot produce the correct widths and energy positions of quasilocalized d bands. Hence, the GGA calculated edges of the optical conductivity are shifted towards smaller energies as compared to the experiment in all noble metals. The inclusion of the correlation effects, which have been done in this work by using GGA+U approximation, substantially improves the description of the optical spectra of noble metals not only in the energy position of the edge of the optical conductivity spectra, but also in the absolute value and the shape of the spectra.

Although all three noble metals have very similar energy band structures, the nature of their MO properties is quite different. Our first-principles band structure calculations show that the shape of Kerr spectra in Ag results mostly from the resonance structure of the function $[\omega \mathrm{D}(\omega)]^{-1}$, so the sharp Kerr effect in Ag is not due to the electronic interband transitions, but rather to the plasma-edge splitting. In the case of Cu, the contributions to the MOKE from the SO interaction and spin magnetic moment are very small and the main effect comes from the orbital contribution to the Zeeman term suppressed to some extent by the diamagnetic contribution of core and valence electrons. Therefore, Cu belongs to a very seldom class of materials where the MO properties are fully determined by the orbital motion of the valence electrons.

The GGA+U calculations reproduce the experimentally observed Cu, Ag, and Au MOKE spectra in a very satisfactory way and explain their microscopic origin. The band-by-band and the **k**-space decomposition of noble-metal MO spectra have been performed and the transitions responsible for the prominent structures in the spectra identified. The dominant contribution which determines the characteristic shape of the spin-part contribution to the σ_{2xy} spectrum of noble metals comes from the $3,4,5 \rightarrow 6$ interband transitions. Although the orbital-part interband transitions in noble metals are formed almost entirely by the same $3,4,5 \rightarrow 6$ transitions, there is a significant difference between the spin and orbital interband transitions. The orbital interband transitions are more smooth functions of energy and cover a whole energy interval for all the $n \rightarrow m$ transitions. To see how the interband transitions between the individual bands are located in the reciprocal space of noble metals, we performed the **k**-space decomposition of the spin and orbital interband transitions into transitions occurring in the vicinity of the high-symmetry points of the Brillouin zone. We found that the main magneto-optical activity of noble metals in the UV-Vis spectral range originates from transitions in the small-volume regions of Brillouin zone near the neck and belly of the Fermi surface in vicinity of X and L high-symmetry points.

ACKNOWLEDGMENTS

The authors are thankful to Dr. A. N. Yaresko for significant contribution to this work at an early stage and for the helpful discussions later. V.N.A. gratefully acknowledges the hospitality during his stay at the University of Bialystok.

[1] E. G. Maksimov, I. I. Mazin, S. N. Rashkeev, and Y. A. Uspenskii, J. Phys. F: Met. Phys. **18**, 833 (1988).
[2] H. U. Yang, J. D'Archangel, M. L. Sundheimer, E. Tucker, G. D. Boreman, and M. B. Raschke, Phys. Rev. B **91**, 235137 (2015).
[3] V. N. Antonov, A. I. Bagljuk, A. Y. Perlov, V. V. Nemoshkalenko, V. N. Antonov, O. K. Andersen, and O. Jepsen, Fiz. Nizk. Temp. **19**, 689 (1993).
[4] R. L. Olmon, B. Slovick, T. W. Johnson, D. Shelton, S. H. Oh, G. D. Boreman, and M. B. Raschke, Phys. Rev. B **86**, 235147 (2012).
[5] K. Stahrenberg, T. Herrmann, K. Wilmers, N. Esser, W. Richter, and M. J. G. Lee, Phys. Rev. B **64**, 115111 (2001).
[6] J. C. McGroddy, A. J. McAlister, and E. A. Stern, Phys. Rev. **139**, A1844 (1965).
[7] S. E. Schnatterly, Phys. Rev. **183**, 664 (1969).
[8] E. Huber and E. Marinero, Appl. Phys. A **A47**, 131 (1988).
[9] J. Cerne, D. C. Schmadel, M. Grayson, G. S. Jenkins, J. R. Simpson, and H. D. Drew, Phys. Rev. B **61**, 8133 (2000).
[10] S.-H. Deng, S.-Y. Wang, J. Li, Z. Liu, Y.-L. Chen, Y.-M. Yang, L.-Y. Chen, H. Liu, X.-X. Zhang, and D. Lynch, Acta Phys. Sin. **50**, 169 (2001).
[11] G.-M. Choi, B.-C. Min, K.-J. Lee, and D. G. Cahill, Nature Commun. **5**, 4334 (2014).
[12] G.-M. Choi and D. G. Cahill, Phys. Rev. B **90**, 214432 (2014).
[13] G.-M. Choi, C.-H. Moon, B.-C. Min, K.-J. Lee, and D. G. Cahill, Nat. Phys. **11**, 576 (2015).
[14] M. Berritta, R. Mondal, K. Carva, and P. M. Oppeneer, Phys. Rev. Lett. **117**, 137203 (2016).
[15] N. E. Christensen and B. O. Seraphin, Phys. Rev. B **4**, 3321 (1971).
[16] P. Heimann and H. Neddermeyer, J. Phys. F: Met. Phys. **7**, L37 (1977).
[17] A. C. Maggs and N. W. Ashcroft, Phys. Rev. Lett. **59**, 113 (1987).
[18] V. P. Zhukov, F. Aryasetiawan, E. V. Chulkov, I. G. de Gurtubay, and P. M. Echenique, Phys. Rev. B **64**, 195122 (2001).
[19] A. Marini, G. Onida, and R. DelSole, Phys. Rev. Lett. **88**, 016403 (2001).
[20] A. Marini, C. Hogan, M. Gruening, and D. Varsano, Comput. Phys. Commun. **180**, 1392 (2009).
[21] Z. Yi, Y. Ma, M. Rohlfing, V. M. Silkin, and E. V. Chulkov, Phys. Rev. B **81**, 125125 (2010).
[22] T. Rangel, D. Kecik, P. E. Trevisanutto, G.-M. Rignanese, H. VanSwygenhoven, and V. Olevano, Phys. Rev. B **86**, 125125 (2012).
[23] A. N. Yaresko, L. Uba, S. Uba, A. Y. Perlov, R. Gontarz, and V. N. Antonov, Phys. Rev. B **58**, 7648 (1998).
[24] L. Uba, S. Uba, V. N. Antonov, A. N. Yaresko, and R. Gontarz, Phys. Rev. B **62**, 16510 (2000).

[25] W. Reim and J. Schoenes, in *Ferromagnetic Materials*, edited by E. P. Wohlfarth and K. H. J. Buschow (North-Holland, Amsterdam, 1990), Vol. 5, p. 133.
[26] J. Schoenes, in *Electronic and Magnetic Properties of Metals and Ceramics*, edited by R. W. Cahn, P. Haasen, and E. J. Kramer (Verlag Chemie, Weinheim, 1992), Vol. 3A of Materials Science and Technology, p. 147, volume edited by K. H. J. Buschow.
[27] H. S. Bennet and E. A. Stern, Phys. Rev. **137**, A448 (1965).
[28] R. Kubo, J. Phys. Soc. Jpn. **12**, 570 (1957).
[29] C. S. Wang and J. Callaway, Phys. Rev. B **9**, 4897 (1974).
[30] V. Antonov, B. Harmon, and A. Yaresko, *Electronic Structure and Magneto-Optical Properties of Solids* (Kluwer, Dordrecht, 2004).
[31] G. E. Grechnev, N. V. Savchenko, I. V. Svechkarev, M. J. G. Lee, and J. M. Perz, Phys. Rev. B **39**, 9865 (1989).
[32] V. N. Antonov, L. Uba, S. Uba, A. N. Yaresko, A. Y. Perlov, and V. V. Nemoshkalenko, Low Temp. Phys. **27**, 425 (2001).
[33] V. N. Antonov, B. N. Harmon, and A. N. Yaresko, Phys. Rev. B **63**, 205112 (2001).
[34] L. Uba, S. Uba, V. N. Antonov, A. N. Yaresko, and R. Gontarz, Phys. Rev. B **64**, 125105 (2001).
[35] L. Uba, S. Uba, V. N. Antonov, A. N. Yaresko, T. Slezak, and J. Korecki, Phys. Rev. B **62**, 13731 (2000).
[36] V. N. Antonov, O. Jepsen, A. N. Yaresko, and A. P. Shpak, J. Appl. Phys. **100**, 043711 (2006).
[37] V. N. Antonov, B. N. Harmon, A. N. Yaresko, and A. P. Shpak, Phys. Rev. B **75**, 184422 (2007).
[38] V. P. Antropov, V. N. Antonov, L. V. Bekenov, A. Kutepov, and G. Kotliar, Phys. Rev. B **90**, 054404 (2014).
[39] O. K. Andersen, Phys. Rev. B **12**, 3060 (1975).
[40] A. Y. Perlov, A. N. Yaresko, and V. N. Antonov, *PY-LMTO, A Spin-polarized Relativistic Linear Muffin-tin Orbitals Package for Electronic Structure Calculations* (unpublished).
[41] V. V. Nemoshkalenko, A. E. Krasovskii, V. N. Antonov, V. N. Antonov, U. Fleck, H. Wonn, and P. Ziesche, Phys. Status Solidi B **120**, 283 (1983).
[42] J. P. Perdew and Y. Wang, Phys. Rev. B **45**, 13244 (1992).
[43] J. P. Perdew, K. Burke, and M. Ernzerhof, Phys. Rev. Lett. **77**, 3865 (1996).
[44] P. E. Blöchl, O. Jepsen, and O. K. Andersen, Phys. Rev. B **49**, 16223 (1994).
[45] P. B. Johnson and R. W. Christy, Phys. Rev. B **6**, 4370 (1972).
[46] W. John, V. V. Nemoshkalenko, V. N. Antonov, and V. N. Antonov, Phys. Status Solidi B **121**, 233 (1984).
[47] V. N. Antonov, Solid State Commun. **51**, 723 (1984).
[48] A. V. Zhalko-Titarenko, M. L. Evlashina, V. V. Nemoshkalenko, and V. N. Antonov, Phys. Status Solidi B **175**, 389 (1993).
[49] V. Frank, Appl. Sci. Res. **B7**, 41 (1958).
[50] J. P. Perdew and A. Zunger, Phys. Rev. B **23**, 5048 (1981).
[51] V. I. Anisimov, J. Zaanen, and O. K. Andersen, Phys. Rev. B **44**, 943 (1991).
[52] L. Hedin, Phys. Rev. **139**, A796 (1965).
[53] W. Metzner and D. Vollhardt, Phys. Rev. Lett. **62**, 324 (1989).
[54] T. Pruschke, M. Jarell, and J. K. Freericks, Adv. Phys. **44**, 187 (1995).
[55] A. Georges, G. Kotliar, W. Krauth, and M. J. Rozenberg, Rev. Mod. Phys. **68**, 13 (1996).
[56] A. N. Yaresko, V. N. Antonov, and P. Fulde, Phys. Rev. B **67**, 155103 (2003).
[57] V. I. Anisimov and O. Gunnarsson, Phys. Rev. B **43**, 7570 (1991).
[58] I. V. Solovyev, P. H. Dederichs, and V. I. Anisimov, Phys. Rev. B **50**, 16861 (1994).
[59] P. H. Dederichs, S. Blügel, R. Zeller, and H. Akai, Phys. Rev. Lett. **53**, 2512 (1984).
[60] W. E. Pickett, S. C. Erwin, and E. C. Ethridge, Phys. Rev. B **58**, 1201 (1998).
[61] M. Cococcioni and S. de Gironcoli, Phys. Rev. B **71**, 035105 (2005).
[62] K. Nakamura, R. Arita, Y. Yoshimoto, and S. Tsuneyuki, Phys. Rev. B **74**, 235113 (2006).
[63] F. Aryasetiawan, M. Imada, A. Georges, G. Kotliar, S. Biermann, and A. I. Lichtenstein, Phys. Rev. B **70**, 195104 (2004).
[64] I. V. Solovyev and M. Imada, Phys. Rev. B **71**, 045103 (2005).
[65] F. Aryasetiawan, K. Karlsson, O. Jepsen, and U. Schonberger, Phys. Rev. B **74**, 125106 (2006).
[66] G.-Q. Liu, V. N. Antonov, O. Jepsen, and O. K. Andersen, Phys. Rev. Lett. **101**, 026408 (2008).
[67] M. Guerrisi, R. Rosei, and P. Winsemius, Phys. Rev. B **12**, 557 (1975).
[68] H. Ehrenreih and H. R. Philipp, Phys. Rev. **128**, 1622 (1962).